Effect of Dispersed Particles on Buoyant Plumes in Stratified Environments

Harish N Mirajkar[1], Sridhar Balasubramanian[2,*]

[1]Research Scholar, Department of Mechanical Engineering, Indian Institute of Technology Bombay, Mumbai, India
[2]Assistant Professor, Department of Mechanical Engineering, Indian Institute of Technology Bombay, Mumbai, India
*corresponding author: sridharb@iitb.ac.in

Abstract: Particle-laden plumes occur in many industrial, and environmental engineering flows. Some examples include gaseous emissions into the atmosphere, liquid effluents discharged into rivers, volcanic eruptions, and hydrothermal flows at the bottom of the ocean. In this present study, laboratory experiments were conducted to study the dynamics of dispersed particle-laden plume produced by a constant inflow into a linearly stratified medium. Particles having mean size, d_p=100 μm, density ρ_p=2500 kg/m^3 were injected along with the lighter buoyant fluid into stratified environment having a stratification strength N=0.67s^{-1}. The effect of low volume fractions, Φ_v=0.35%, 0.5% and 0.7%, of particles on the plume particle cloud, defined as distance of the plume from the neutral buoyant layer or spreading height, was measured and its effect on the radial intrusion of plume was studied. The radial spreading rate, R_f, for a particle-laden plume in the inertia-buoyancy regime advanced in time as $R_f \propto t^{2/3\pm0.02}$, which is lower compared to the no particle case. The effect of particles on thickness of the plume, h_p, was also studied and was found to be lower than the no particle case. Additionally, plume shape profile near the neutral buoyant layer for different volume fractions was studied to get a better understanding of the plume evolution in the presence of particles.
Keywords: plume, particle cloud, inertia-buoyancy regime, plume thickness.

1 Introduction

In environmental and engineering flows, the scalar transport of species occurs in form of jets and plumes. Some examples include release of gases during volcanic eruptions, gravity currents, ocean fresh water overflows, and effluent discharges [1].These processes almost always have small quantities of particles that govern their flow behavior. Moreover, these fluid motions are modified in the presence of a stratified, density varying ambient environment. It is therefore imperative to quantify the turbulent mixing behavior, fluid entrainment, and the transition from jet to plume phases in a density stratified environment to accurately model these geophysical processes. A jet motion has a dominant momentum phase, whereas the plume motion has a dominant buoyancy phase that creates an upward motion of the fluid away from the source. If one considers a stratified or density varying environment, then the jet behaves as a forced plume that has both initial momentum as well as buoyancy. As this forced plume evolves in space and time, it becomes a pure plume which is solely dominated by buoyancy. Depending on the ratio on $(M_0/B_0)N^{1/2}$, one can demarcate the jet, forced plume and pure plume regimes, where M_0, B_0 and N are the initial momentum flux, initial buoyancy flux, and Brunt Vaisala frequency, defined as follows [2];

$$B_0 = g\left(\frac{\rho - \rho_a}{\rho_a}\right)Q_0 = g' Q_0$$

$$M_0 = Q_0 w_0$$

$$Q_0 = \frac{1}{4}\pi d^2 w_0$$

$$N = \sqrt{\frac{g}{\rho_0}\frac{d\rho}{dz}}$$

Where ρ_a is the density of ambient, ρ is the jet density, ρ_0 is some reference density, d is the jet diameter and w_0 is the initial vertical velocity. Now, if $(M_0/B_0)N^{1/2}<0.1$, then the flow behaves as a pure plume, $(M_0/B_0)N^{1/2}>2$, it is jet dominated, and for intermediate values of $(M_0/B_0)N^{1/2}$, the flow is a forced plume. Depending on the regime, the entrainment of the fluid with the ambient fluid is also different, and is characterized by "entrainment coefficient", α, first introduced by Morton et al. [3]. The mixing dynamics of

stratified flows was initially studied by Schmidt [14] and Morton, Taylor & Turner in 1956 [8]. Since then, numerous research studies have been done on this topic [1, 5, 8, 9, 16]. Most of the early work on this topic was based on similarity theory using the governing equations for stratified flows, namely conservation of mass, momentum and density along with the Boussinesq approximation [8]. The bulk parameters such as maximum height, Z_H, defined as the height at which the vertical velocity vanishes, has been measured in different studies, and empirically related to the entrainment coefficient using self similar arguments [3]. In all of these studies, other plume parameters such as plume radial propagation, thickness etc. has been ignored, and only recent studies have measured these parameters [3, 10]. Although explosive volcanic eruptions are rich in particles of a wide range of sizes (e.g., pumice and ash), few studies address the influence of particles on the mechanics of entrainment and mixing [2, 3, 12]. The entrained particles impart additional inertial and buoyancy effects and change the evolution and growth of the plume. The particles influence on the entrainment and plume growth depends on the extent to which they are coupled to the flow. In this communication, we will present results from experiments conducted to study the effect of low particle concentrations on the plume behavior. In particular, we will focus on the radial propagation, plume thickness, plume profile, and formation of a particle cloud. These results will be compared with the single-phase case, and the differences would be subjected to physically explanations.

2 Experimental Conditions

Experiments for studying plume dynamics and mixing were performed in a two tank facility, the schematic of which is shown in Figure 1. The setup primarily consists of two acrylic tanks, one for storing the jet fluid, and the other for storing the ambient fluid. The tank comprising of the jet fluid, henceforth referred to as T1, is 0.6x0.6x0.6 m and filled with water, with ρ=999 kg/m^3. The second tank henceforth referred to as T2, with dimensions of 0.91m long by 0.91m wide by 0.6m high was used for storing the ambient linearly stratified fluid. A double bucket system was used for creating a linear stratification in the tank, T2. In the two bucket system**,** two buckets made are connected with a control valve, with one bucket filled with salt solution of required density, and the other filled with water (ρ_b=999 kg/m^3 at temperature, T=25^{0}C). Once a steady state is reached, the valve is opened allowing the higher density fluid to flow. This creates a pressure difference, ∇P, and water from the second bucket flows into the first bucket, and we slowly achieve a linear stable stratification (dρ/dz <0). The linearity of the profile was checked using a Delta-Ohm (model HD 2106) conductivity probe. A typical density profile is shown in Fig 2.

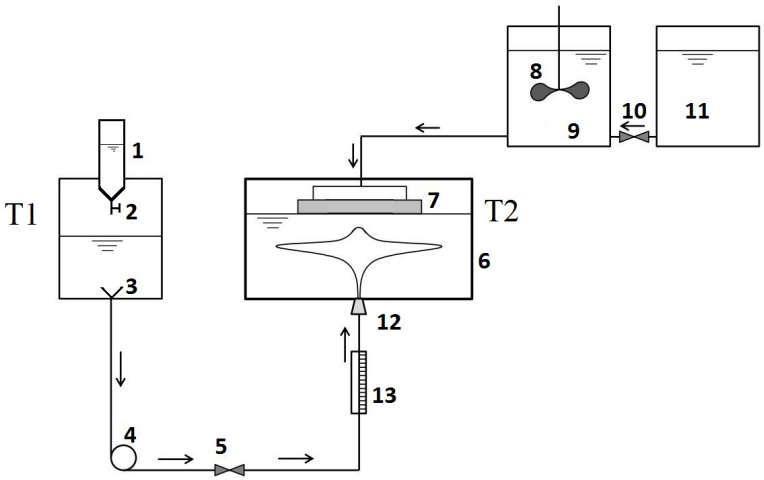

Fig.1: Schematic of experimental setup. 1. Conical particle feeder, 2,5,10. Control valve, 3. Funnel, 4. Centrifugal pump, 6. Stratification tank (T2), 7. Wooden plate, 8. Fluid mixer, 9. Salt water bucket, 11. Fresh water bucket, 12. Jet nozzle, 13. Flowmeter.. Dimensions of the tank are given in the text in Sec. 2.

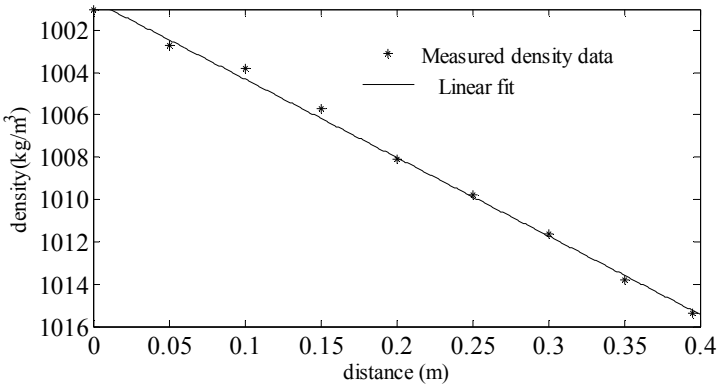

Fig 2: Density profile in the stratification tank measured using the conductivity probe

A centrifugal pump, shown in Figure 1, was used to discharge the jet fluid into the ambient linearly stratified environment using a round jet nozzle seated at the bottom of the tank. The jet nozzle was 160 mm in length with diameter, d=12.7 mm, and was made of aluminum, composed of diffuser, settling chamber, and contraction sections. It was designed on the principle discussed by Mehta and Bradshaw [7] for designing a wind tunnel. A honeycomb was placed in the settling chamber to reduces the flow fluctuation (≈3-5% in the present experiments) and generate stable flow at the nozzle exit. A linear stable stratification with water and commercial salt (NaCl) was obtained in T2, such that heavy fluid at the bottom and light fluid is at the top. The jet fluid (water) from the T1 was pumped into the main tank (T2) using centrifugal pump. The volumetric flow rate was controlled with a needle valve in the flow meter. Three sets of experiments were conducted for different particle volume fraction for a fixed value of $N=0.67$. For each volume fraction, i.e., Φ_v=0.35%, 0.5%, and 0.7%, the experiment was repeated five to seven times to get a statistical ensembles. The stratification profile was measured using a conductivity probe, and it was seen that in all the experiments the profile was linear with an error estimate of ±2%. The flow dynamics were captured using food dye in the high resolution digital and video camera. Two cameras were fitted, one from the top and one from the side to record the flow dynamics in the x-z plane (side view) and x-y plane (top view). The recording was converted into images from these images the flow parameters, such as radial propagation, plume thickness, plume profile, and parabolic cloud patterns were measured as shown in figure 3. Additionally the effect of particles on each of the above mentioned parameter was measured and compared with the single-phase plume. The uncertainty involved in the image measurement was within ±2%.

3 Results and Discussion

In this section, the results from the experiments will be discussed for both single-phase plume for which Φ_v=0%, and the particle-laden case where Φ_v varies from 0.35% to 0.7%. The parameters that were measured in our present experiment are discussed below. A schematic explaining their definition is shown in Fig.3 Below we present in detail the variation of these parameters for single-phase and multi-phase plume.

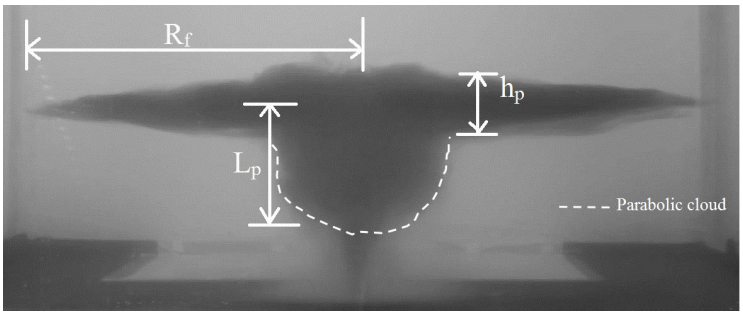

Fig 3 Schematic representation of experimental parameters for multi-phase plume for the Φ_v = 0.5% at time t=70sec

1. *Radial intrusion of plume (R_f)*: It is refers to the horizontal motion of the plume after trapping at the neutral buoyant layer. Due to the inertia, the plume moves horizontally once it encounters the neutral buoyant layer. The radial propagation was studied in a linear stratified medium for both single-phase and particle-laden plume. The results of plume spread for different values of volume fraction, ϕ_v, is shown in Fig 4. It was observed from the experiments that particle-laden plume follows four different growth regimes, namely, (i) Radial momentum balanced by inertia, (ii) Inertia-buoyancy regime, (iii) Fluid-particle inertia regime, and (iv) viscous-buoyancy regime. The regime (iii) was absent for the case of single-phase plume which is consistent with previous studies [6, 10]. From the figure it is clear that for a particle-laden plume in the inertia buoyancy regime, the propagation is $R_f \alpha\ t^{0.68}$, where for a single phase plume $R_f \alpha\ t^{0.75}$. Thus, the radial propagation speed of particle-laden plume is slower compared to the single-phase plume, which could be attributed to the parabolic cloud formation. More finer details on the effect of particles on plume radial intrusion could be found in *Harish et al.* [3].

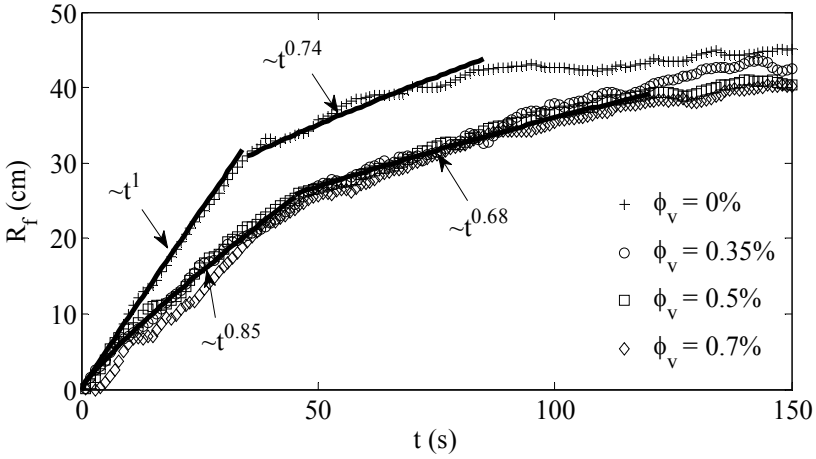

Fig 4: Radial distance, R_f, of the intrusion front from the plume centerline as a function of time

2. *Plume thickness (h_P)*: As the plume radially propagates, due to the buoyancy effects, the plume also spreads vertically, thereby increasing its thickness (see Figs 5, 6). Such a plume spread is referred to as 'coning', where the plume expands both in horizontal and vertical directions, and is a common feature of a mixing plume. Thus, along with the radial propagation, the thickness of the plume can also be measured and is shown in fig. 5 at a point denoted as R_1. This point R_1 is a point after which the inertia-buoyancy regime is encountered. As seen in the figure, at R_1, the plume thickness increases due to initial transient and then reaches a steady value. The steady state plume thickness for Φ_v=0% is h_p = 11.0±0.5cm. A similar result was observed by [10] in their work on single-phase plume. In the case of particle-laden plume, we observed the same characteristics as that of single-phase plume, but with a slight decrease in the constant value h_p = 8.5±0.5cm at point R_1. Surprisingly, this value was almost same (±0.5%) for all the three volume fractions (Φ_v = 0.35%, 0.5% and 0.7%) An interesting point to note is that the particle-laden plume has a lower thickness compared to the single phase case, and hence the presence of particles has some effect of the plume behavior. The lower in the h_p in the particle-laden case can be attributed due to the presence of the plume in the particle cloud below the neutral layer reducing the plume propagation compare to single phase plume [3]. Considering a point further away from R_1, i.e. at a radial distance of r=12.5 cm from R_1, it was found that the plume thickness, h_p, never reached a steady value. This is shown in Fig 6, where we observe that h_p increases with time. The rate of increase in the plume thickness seemed to follow a power law: for $\Phi_v = 0$, $h_p \alpha\ t^{0.45\pm0.02}$ and for $\Phi_v > 0\%$, $h_p \alpha\ t^{0.38\pm0.02}$

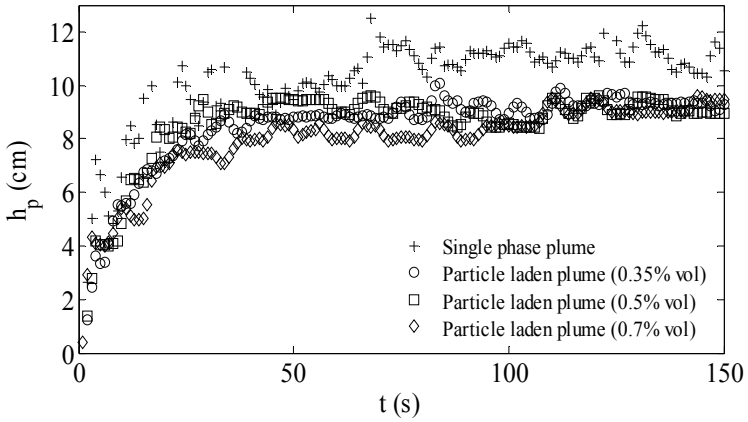

Fig 5: Plot of the intrusion thickness (at position R_1) versus time

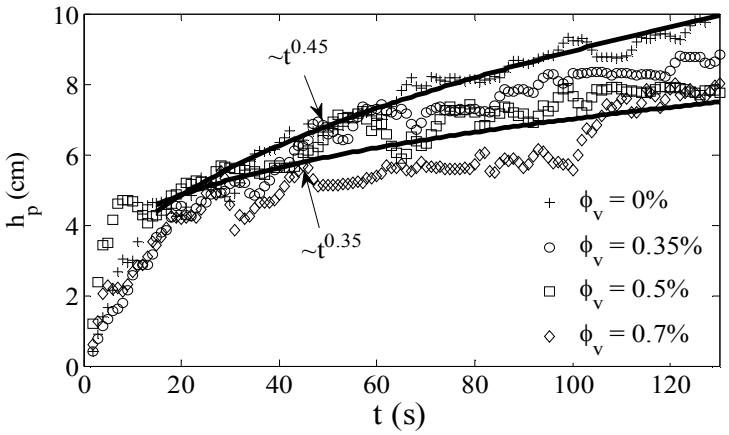

Fig 6: Plot of the intrusion thickness versus time at a radial distance r=12.5 cm from R_1

3. *Plume profiles*: The profile of the plume was plotted using an intensity threshold algorithm as the plume spreads at the neutral buoyant or spreading layer (Z_s). The profile was plotted for a particle-laden plume at different times during the plume evolution and the results are shown in fig 7. As seen from this figure, for all the three volume fractions, ϕ_v, with increase in time, the trough of the profile increases as expected due to the presence of negatively buoyant particles. Interesting point to note is that at low volume fraction (ϕ_v=0.35%), the particle trough reaches a steady state at early time (i.e. the profile doesn't change after t≈80 seconds) compared to the high volume fraction case (ϕ_v=0.5% and 0.7%). As the volume fraction, ϕ_v, increases the profile becomes shallower and at any given time the particle trough is highest for the higher ϕ_v. The extent of particle distribution in the radial direction was found to be the same for all the three volume fractions, which indicates that the particles get collected in a circular pattern at a distance of r=12cm from the center of the nozzle on either sides. The particle distribution after the end of the experiment was found to be symmetric. More analysis needs to be done to understand the reason for such a distribution near, and its independence on the volume fraction.

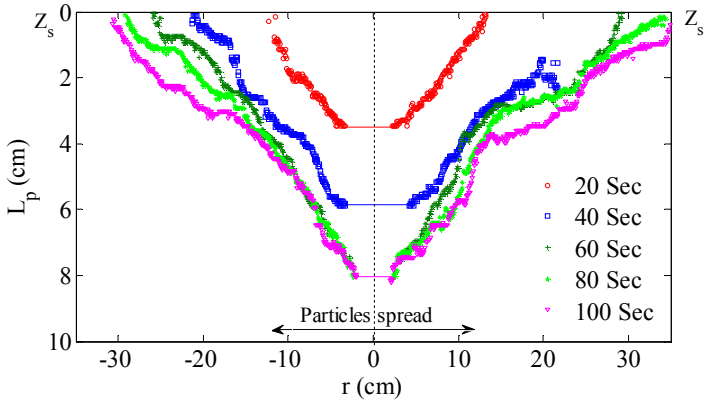

(a)

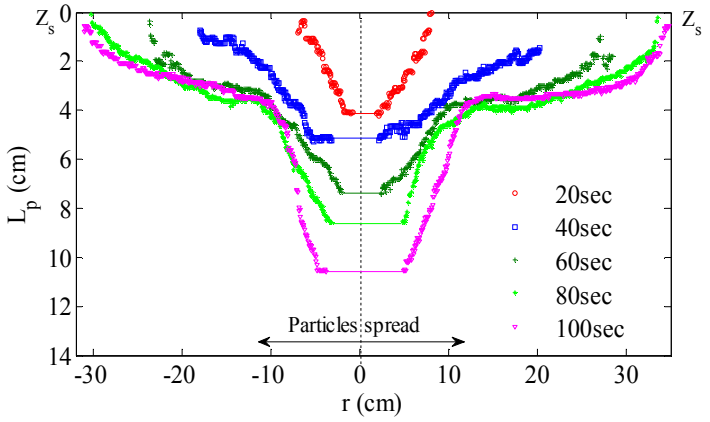

(b)

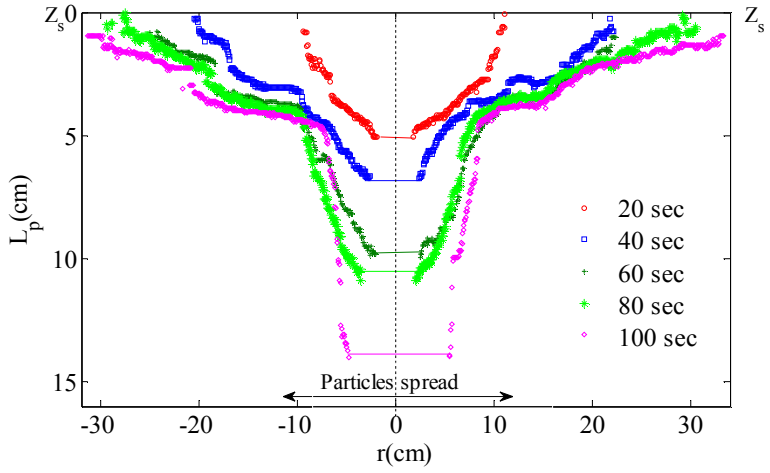

(c)

Figure 7:Evolution of parabolic cloud (L_p) versus radial distance, r from the mean spreading height Z_s for the three different volume fraction, (a)0.35% (b)0.5% (c)0.7%.(Inside) the figure indicates the particles spread, post experiment.

4. *Parabolic cloud (L_P)*: The parabolic cloud is defined as the region below the neutral buoyant or spreading layer where the 'particle fall out' phenomenon occurs [3]. As the particles lose their momentum, they fall out from the neutral buoyant layer and in this process drag the plume downwards. The distance from the mean spreading height (Z_s) to the tip of the trough is used to calculate the extent of L_P. The variation of L_P (vs) volume fraction (ϕ_V) is shown in Fig.8. As seen in this figure as ϕ_V increases the value of L_P also increases. This makes sense since as we increase the particle loading the plume is dragged further downwards by the particles and hence parabolic cloud is much thicker.

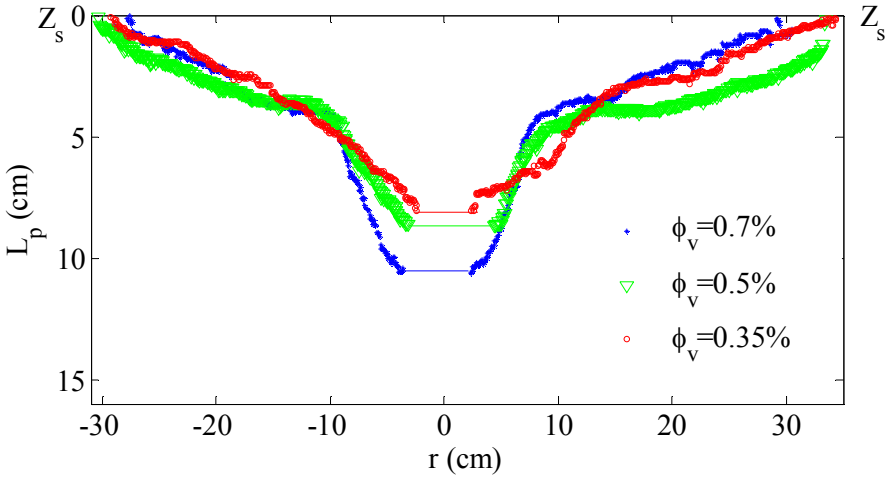

Fig 8: Plot shows the variation of parabolic cloud (L_p) versus radial distance, r at time 80s for the three different volume fraction

4 Conclusions

In the present study, the effect of particles on the radial intrusion of plume, plume thickness, parabolic cloud, and plume profiles were studied. We found from the experiments that in presence of particles the radial propagation of plume(R_f) with time was found follow approximately $t^{2/3}$ power law where as in the absence of particles the R_f followed $t^{3/4}$ power law that is consistent with earlier experiments [6,10]. The power law behavior in the case of particle laden plume from our present experiment was found to be approximately consistent with the satellite observation of Mount Pinatubo eruption plume [4]. Secondly, the plume thickness was compared in the presence/absence of particles, and it was experimentally found that in the case of the particle laden plume, the thickness was lower compared to the no particle case. The reduced thickness in the particle laden case can be attributed due to presence of the parabolic cloud below the neutral layer. Thirdly, the evolution of parabolic cloud profile with time was studied for the three different volume fraction it was found with increase in time, In the case of higher volume fraction with further increase in the time (>100s) the parabolic trough was found to move towards the source of the jet and leads to the secondary umbrella structure [3]. For the given time, the parabolic cloud height was found to increase with the volume fraction *($L_{p0.7} > L_{p0.5} > L_{p0.35}$)*. Particle spread after end of the experiments revealed particle distribution that extended up to r=12cm from the center of the jet. Furthermore experiments are in the progress to understand the behavior of parabolic cloud and particle spreading with initial source jet conditions.

Acknowledgments

The authors acknowledge funding from Department of Science and Technology, and Ministry of Earth Sciences, India for funding the present research work.

References

[1] Ai, Jiaojian et al (2006), "On Boussinesq and non-Boussinesq starting forced plumes." *Journal of Fluid Mechanics,* 558 pp 357-386.

[2] Carey, S. N., H. Sigurdsson, and R. S. J. Sparks (1988), Experimental studies of particle-laden plumes, *J. Geophys. Res*., 93, pp 15,314 – 15,328

[3] Harish N Mirajkar, Siddhesh Tirodkar, Sridhar Balasubramanian (2015) Experimental Study on Growth and Spread of Dispersed Particle-Laden Plume in a Linearly Stratified Environment, *Environment Fluid Mechanics* (DOI: 10.1007/s10652-015-9412-5).

[4] Holasek, R. E., Self, S., & Woods, A. W. (1996). Satellite observations and interpretation of the 1991 Mount Pinatubo eruption plumes. *Journal of Geophysical Research: Solid Earth (1978–2012)*, *101*(B12),pp 27635-27655.

[5] Kumagai, M. (1984). Turbulent buoyant convection from a source in a confined two-layered region. *Journal of Fluid Mechanics*, *147*, pp 105-131.

[6] Kotsovinos, N. E. (2000). Axisymmetric submerged intrusion in stratified fluid. *Journal of Hydraulic Engineering*, *126*(6), pp 446-456.

[7] Mehta, R. D., & Bradshaw, P. (1979). Design rules for small low-speed wind tunnels. *Aeronautical Journal*, *83*(827), 443-449.

[8] Morton, B. R., Taylor, G., & Turner, J. S. (1956). Turbulent gravitational convection from maintained and instantaneous sources. *Proceedings of the Royal Society of London. Series A. Mathematical and Physical Sciences*,*234*(1196), pp 1-23.

[9] Mott, R. W., & Woods, A. W. (2009). On the mixing of a confined stratified fluid by a turbulent buoyant plume. *Journal of Fluid Mechanics*, *623*, 149-165.

[10] Richards, T. S., Aubourg, Q., & Sutherland, B. R. (2014). Radial intrusions from turbulent plumes in uniform stratification. *Physics of Fluids,26*(3), 036602.

[11] Rooney, G. G.; Devenish, B. J. Plume rise and spread in a linearly stratified environment, *Geophysical & Astrophysical Fluid Dynamics*, vol. 108, issue 2, pp. 168-190

[12]Veitch, G., & Woods, A. W. (2002). Particle recycling in volcanic plumes. *Bulletin of volcanology*, *64*(1), 31-39.

[13] Oster, G., & Yamamoto, M. (1963). Density Gradient Techniques. *Chemical Reviews*, *63*(3), 257-268

[14] Schmidt, W. (1941). Turbulente ausbreitung eines stromes erhitzter luft.*ZAMM-Journal of Applied Mathematics and Mechanics*, *21*(5), pp 265-278.

[15] Turner, J. S, (1979) “Buoyancy Effects in Fluids”. Cambridge University Press

[16] Turner, J.S. (1986). “Turbulent entrainment: the development of the entrainment assumption, and its application to geophysical flows”. *Journal of Fluid Mechanics*, *173*(431), pp 71.